Published in final edited form as:
IEEE Trans Ultrason Ferroelectr Freq Control. 2011 July ; 58(7): 1406–1417. doi:10.1109/TUFFC.2011.1960.

The Feasibility of Using Thermal Strain Imaging to Regulate Energy Delivery During Intracardiac Radio-Frequency Ablation

Chi Hyung Seo[Member, IEEE],
University of Washington, Department of Bioengineering, Seattle, WA

Douglas N. Stephens[Member, IEEE],
University of California, Davis, Department of Biomedical Engineering, Davis, CA

Jonathan Cannata[Member, IEEE],
University of California, Davis, Department of Biomedical Engineering, Davis, CA

Aaron Dentinger[Member, IEEE],
GE Global Research, Imaging Technologies, Niskayuna, NY

Feng Lin[Member, IEEE],
GE Healthcare, Wuxi, China

Suhyun Park,
GE Global Research, Imaging Technologies, Niskayuna, NY

Douglas Wildes[Senior Member, IEEE],
GE Global Research, Imaging Technologies, Niskayuna, NY

Kai E. Thomenius[Member, IEEE],
GE Global Research, Imaging Technologies, Niskayuna, NY

Peter Chen,
St. Jude Medical, Irvine, CA

Tho Nguyen,
St. Jude Medical, Irvine, CA

Alan de La Rama,
St. Jude Medical, Irvine, CA

Jong Seob Jeong[Member, IEEE],
Dongguk University-Seoul, Seoul, South Korea

Aman Mahajan,
UCLA Medical Center, Los Angeles, CA

Kalyanam Shivkumar,
UCLA Medical Center, Los Angeles, CA

Amin Nikoozadeh[Student Member, IEEE],
Stanford University, Stanford, CA

Omer Oralkan[Senior Member, IEEE],
Stanford University, Stanford, CA

Uyen Truong,
University of Colorado, Aurora, CO

David J. Sahn,
Oregon Health and Science University, Cardiology, Portland, OR

Pierre T. Khuri-Yakub[Fellow, IEEE], and

Stanford University, Electrical Engineering, Stanford, CT

Matthew O'Donnell[Fellow, IEEE]
University of Washington, Department of Bioengineering, Seattle, WA

Abstract

A method is introduced to monitor cardiac ablative therapy by examining slope changes in the thermal strain curve caused by speed of sound variations with temperature. The sound speed of water-bearing tissue such as cardiac muscle increases with temperature. However, at temperatures above about 50° C, there is no further increase in the sound speed and the temperature coefficient may become slightly negative. For ablation therapy, an irreversible injury to tissue and a complete heart block occurs in the range of 48 to 50°C for a short period in accordance with the well-known Arrhenius equation. Using these two properties, we propose a potential tool to detect the moment when tissue damage occurs by using the reduced slope in the thermal strain curve as a function of heating time. We have illustrated the feasibility of this method initially using porcine myocardium *in vitro*. The method was further demonstrated *in vivo*, using a specially equipped ablation tip and an 11-MHz microlinear intracardiac echocardiography (ICE) array mounted on the tip of a catheter. The thermal strain curves showed a plateau, strongly suggesting that the temperature reached at least 50°C.

I. Introduction

Catheter ablation has become a significant modality to manage cardiac arrhythmias [1]–[5]. It has transformed the field of cardiac electrophysiology from a diagnostic tool to a potent prophylactic and curative method. An exciting recent development is the increasing adoption of catheter ablation for atrial fibrillation [6]. Atrial fibrillation is the most frequent arrhythmia in clinical practice and its incidence is increasing as the population ages [7].

Radio-frequency ablation (RFA) is used in electrophysiology (EP) procedures to permanently alter the myocardium in locations which support aberrant electrical conduction pathways, contributing to irregular heart rhythm. Regulating power to maximize safety and efficacy of energy application is critical for successful outcomes. Currently, the tissue effects of RF delivery can be monitored indirectly by real-time analysis of impedance [8], electrogram amplitude [9], the electrophysiologic behavior of the tissue being ablated [10], and temperature at the tip of the electrode [11], [12], but none provide an accurate indication of tissue temperature during ablation.

Tissue temperature is critically related to the success or failure of catheter ablation procedures [13], [14]. To ensure irreversible injury, a tissue temperature of approximately 50°C must be achieved [13], [14]. The minimum temperature needed to create a complete heart block has been observed to be 48°C [11], [15]. Raising tissue temperature significantly beyond this point can be unnecessary and cause complications during the procedure. High temperature at the tissue site may result in coagulum formation on the electrode, endocardial disruption, steam popping, or perforation. This would lead to an abrupt rise in impedance which would result in a marked decrease in tissue heating [16], [17]. Furthermore, if a coagulum develops, the ablation catheter must be removed, cleaned, and repositioned, necessitating additional catheter manipulation and additional fluoroscopy time.

Because of the importance of temperature monitoring, a standalone thermocouple or a thermistor embedded in the electrode is used during catheter RFA procedures [11], [14]. During energy delivery, a portion of the electrode should be typically in contact with the tissue and the remainder in contact with surrounding blood. The electrode temperature recorded by the thermocouple reflects a complex interaction between the production of heat in nearby tissue

by the radio-frequency field and convective heat loss to surrounding blood and tissue [14], [18]–[20]. Because of convective heat losses, the temperature recorded by the thermocouple could be consistently less than that at the hottest point in the tissue, misleading the operator to increase the energy delivered. An optical fluorometric temperature probe [11], [21], for example, could be used for more sensitive measurement at increased cost and lower speed. In general, temperature sensors are additional devices to be handled and installed in an already crowded catheter tip volume.

Temperature imaging using ultrasound techniques is more attractive because of the potential to provide 2-D real-time temperature information at low cost. However, standard B-mode images are less than optimal for visualizing the response to heating because the targeted region and surrounding tissue usually have similar scattering characteristics. Bright echoes from bubble formation at high temperature are not desirable for ablation monitoring because bubbles imply the tissue temperature has exceeded 50°C, causing coagulum and charring [22].

Even though conventional B-mode images cannot clearly identify regions being treated by RFA, ultrasound signals can provide useful information. For example, several ultrasonic methods have been proposed to estimate temperature changes in tissue. All are related to different temperature-induced changes in the ultrasonic properties of tissue, including frequency-dependent attenuation [23], backscattered power [24], speed of sound [25], thermal expansion [26], or a combination of the last two effects [27], [28]. A tissue differentiation technique, thermal strain imaging (TSI), also has been developed recently, building on this early work in ultrasonic temperature estimation [29]. It uses phase-sensitive speckle tracking to create thermal strain images based on the temperature dependence of sound speed. TSI has already been successfully used in atherosclerosis detection and tissue characterization [29]–[32].

However, ultrasound-based temperature measurement over large ranges is limited because the sensitivity to sound speed changes beyond 50°C is low [33]. If a very high temperature is considered (tissue temperature of 50°C or higher), as in the case of high-intensity focused ultrasound (HIFU), the effect is two-fold: speed-of-sound variations with temperature are not as sensitive and the tissue undergoes state changes that could fundamentally change the ultrasound backscatter signal character. Also, limited data are available for the relationship between temperature and the sound speed of tissues *in vivo*, especially at temperatures above 50°C [22], [24], [26], [33]–[36].

Speed of sound variations with temperature introduce apparent shifts in scatterer position and thermal expansion of the medium introduces a physical shift in scatterer position. Beyond 50°C, thermal expansion is no longer negligible and contributes to the total echo shift or delay in strain calculations [22], [24], [26], [33]–[36]. Thus, thermal strain imaging may not be practical for ablation monitoring based on precise temperature measurements because it is most sensitive and unambiguous for small temperature changes in the temperature range below 50°C. For ablation treatment of arrhythmia, however, a robust, reproducible indicator of tissue necrosis rather than absolute temperature monitoring is required. In particular, it is most important to know when tissue temperature has reached or exceeded 50°C so ablation can be terminated.

It is our hypothesis that by measuring thermally-induced strain as a function of time during the ablation procedure, there will be a point when the slope of the thermally-induced strain approaches zero. That is, by continuously tracking from a reference frame just before the start of ablation, the thermal strain will eventually plateau because the sound speed has reached its maximum value as a function of temperature.

The signal-processing methods proposed in this paper were developed to investigate the feasibility of monitoring ablative therapy by identifying the point at which the magnitude of

the slope of the thermal strain curve decreases significantly, caused primarily by speed of sound variations with temperature. We first test this idea in a dynamic heating experiment using excised porcine myocardium *in vitro*. The feasibility of this method for ablation monitoring is also tested *in vivo*.

II. Methods

A. Dynamic Heating Experiment In Vitro

To ensure that sufficient heat could be delivered for lesion formation, excised porcine heart was prepared in a saline solution. While submerged, the sample was fixed on a holder to minimize any motion. It was then allowed to reach 37°C (taking about 2 h) in a heated saline bath before the experiment began.

RF data were collected using a prototype integrated ablation catheter array interfaced with a GE Vivid 7 imaging system (GE Healthcare, Horten, Norway). The ultrasound transmit frequency was 11 MHz with a transmit focus at 1 to 2 mm. Temperatures in the tissue were measured using an implanted fine-wire thermocouple. Thermocouple, ablation catheter, and sample were positioned as shown in Fig. 1. A digital thermocouple reader was used to record the temperature at 1-s intervals. Table I summarizes relevant ultrasound system parameters used for these *in vitro* experiments, and for subsequent *in vivo* tests described later.

B. Catheter Ablation Experiment In Vivo

For the *in vivo* study, juvenile Yorkshire pigs were used as the animal model. All surgical methods and animal treatment procedures were approved by the Animal Care and Use Committees of the Oregon Health and Science University. All animals were given general anesthesia and maintained with 2% isoflurane and oxygen ventilation. Femoral arteries and veins as well as jugular veins were exposed by surgical incision ready for catheter access. Electrocardiograms, body temperature, and oxygen saturation were continuously monitored. Electrocardiography (ECG) electrodes were connected to the body of the pig for standard three-point recording. The output of the ECG served as the trigger for the Irvine Biomedical Inc. (IBI) generator (St. Jude Medical, Inc., St. Paul, MN). The generator was active for 250 ms beginning at the peak of the ECG R wave, then inactive until the next trigger (Fig. 2). The respirator was stopped during data acquisition (20 s) to reduce undesired motion, such that the dominant physiological motion would be heart motion.

We used a specially designed ultrasound compatible RFA tip integrated into a prototype 9F forward-looking microlinear (ML) ICE catheter array to simultaneously image and ablate the right atrial wall [37], [38]. Additionally, a thermocouple normally residing inside the electrode was pulled out to touch the tissue for thermal strain comparisons. Fig. 3 shows the approximate geometry for this configuration. The transmit frequency was 11 MHz with a transmit focus at 2 mm. Ablation was performed while the integrated imaging and ablation catheter was localized and guided by fluoroscopy.

The electrical impedance during the ablation stayed in the range of 75 to 90 Ω, and the generator indicated that approximately 10 to 40 W were delivered over the 20-s time period. Ablation started after about 5 s of baseline data acquisition.

Continuous ultrasound data were acquired during ablation. Noise from the RF generator did not diminish B-mode image quality.

C. Finite Element Modeling

We have preformed finite element (FE) modeling to visualize the temperature rise and thermal diffusion effects. Temperature rise from RF ablation as a function of time was estimated using an FE representation (COMSOL Multiphysics, v3.2, Comsol, Inc., Burlington, MA) of the bioheat equation [39], [40]

$$\rho C\frac{\partial T}{\partial t}=k\nabla^2 T - W_b C_b(T - T_b)+Q, \quad (1)$$

where k is the thermal conductivity of the tissue (0.533 W/m/K), T is the tissue temperature (K), W_b is the blood perfusion rate (0.013 kg/L/s), C_b is the specific heat of the blood (4180 J/kg/K), C is the specific heat of the tissue (3720 J/kg/K), T_b is the blood temperature (310K), Q is the local power density deposition rate, ρ is the density of the tissue (1060 kg/m^3), and t is time (s) [41]. The accuracy of the power and temperature calculations obtained using the bioheat transfer equation was previously verified elsewhere [42]. A schematic diagram of the modeled region is shown in Fig. 4. The model assumed that the boundary temperature remained at 37°C during the entire procedure. The initial temperature throughout the tissue was 37°C. A portion of the gold electrode was in contact with the blood pool, limiting the extent of the heat delivered to tissue. The RF pulse sequence and exposure duration followed the experimental setup. A 2-D, axially symmetric model was used to reduce computation time. The model consisted of 827 mesh points and 1584 triangular elements.

D. TSI Signal Processing

Because ultrasound data acquisition was not triggered by the ECG, we assumed that the heart returns to its initial state before ablation [43]–[45].

Four frames of data with the least motion were selected by examining B-mode images from the first cardiac cycle before ablation. Using these as reference frames, 2-D cross-correlation was performed to find the best matched frame with the highest cross-correlation (≥0.85) within a cycle for all subsequent cardiac phases. Then, using each frame from the first cardiac cycle as a reference, 2-D speckle tracking was performed with all corresponding frames throughout the experiment. These four displacement sets were averaged to produce the measured axial displacement (Fig. 5).

Two-dimensional phase-sensitive correlation-based speckle tracking [46] was applied to RF data from every frame in the sequence to estimate temporal strain along the axial direction. The tracking algorithm involves calculating complex cross-correlation coefficients between small windowed blocks from two consecutive frames, reducing the probability of peak hopping by filtering the correlation coefficient functions, and estimating the shift from the phase zero-crossing around the peak correlation coefficient. The correlation kernel size was approximately the full-width at half-maximum (FWHM) of a speckle autocorrelation function for optimal strain estimation. Reduced kernel size and correlation filtering significantly decreases peak hopping probability and increases the accuracy of displacement estimation [46].

Axial displacement was estimated from the position of the maximum correlation coefficient, and was further refined using the phase zero-crossing of the complex correlation function. The kernel size used for tracking *in vivo* was slightly larger than the speckle size, approximately 0.3 mm × 6.6° (axial × lateral) and the filter size was 0.75 mm × 7.3° (axial × lateral). Spatial derivatives of the displacements were computed to estimate temporal strain caused by the sound speed change and thermal expansion from axial displacement using a simple 1-D difference filter along the axial direction for correlation windows separated by 0.9 mm.

Finally, thermal strain $(\partial/\partial t)[\delta t(z)]$ is related to sound speed changes and thermal expansion according to

$$\frac{\partial}{\partial t}[\delta t(z)]=(\beta(z)-\lambda(z))\delta\theta(z), \tag{2}$$

where β is the thermal expansion coefficient, λ is the linear coefficient of sound speed versus temperature, and δθ is the temperature change [27]. Thermal expansion can be ignored over a wide range of operating temperatures. λ has a positive value and overwhelms β for water-bearing tissue by at least an order of magnitude until about 50°. At temperatures approaching 50°, thermal expansion cannot be ignored.

III. Results

A. Dynamic Heating Experiment In Vitro

Fig. 6 presents a B-mode overlaid with thermal strain images from the *in vitro* dynamic heating experiment using a prototype PZT ML array for a rapid heating case. For B-mode images, the colorbar represents a standard decibel scale and for strain images, it represents actual (i.e., fractional) strain values. The image presents the thermal strain at approximately 52°C. Several representative pixels in the focal region were averaged to plot the thermal strain as a function of heating time in Fig. 7. The slope changes are noted with gray arrows. Similar results are presented in Figs. 8 and 9 for a slow heating case. For both cases, there is an obvious change in the slope of the thermal strain curve in the region of 50°C.

B. Catheter Ablation Experiment In Vivo

Fig. 10 shows cardiac motion from the four reference frames with no respiratory motion before ablation. The average of a small region about 0.25 mm × 0.1 mm (axial × lateral) used to generate the plots is also highlighted. As expected, motion is minimal because the heart's periodicity enabled the averaging scheme mentioned in the methods section. Figs. 11, 13, and 15 show B-mode and B-mode overlaid with thermal strain images when the thermal strain has reached its maximum magnitude. Figs. 12, 14, and 16 plot the thermal strain versus time. Several representative pixels in the focal region were averaged to plot the thermal strains. Similar to the *in vitro* case, there was a significant slope change around 50°C. Using thermal strain, it was clear when the temperature reaches at least 50°C for the experimental conditions used here. In particular, this method appears promising for the case in which heating is sufficiently fast to minimize the effects of thermal diffusion, as discussed in the next section.

C. Thermal Diffusion Effect

The temperature distribution during RF ablation is affected by two processes: resistive heating from the tip of the electrode and spatial redistribution of heat caused by thermal diffusion. We have compared the temperature rise from one of the *in vivo* data sets to our finite element modeling. Fig. 17 shows that our heating protocol operates in a region where thermal diffusion has not taken over. In particular, the pulse duration for the heating scheme presented in Fig. 2 was sufficiently short that we could assume instantaneous heating of the medium with minimal thermal diffusion. In a clinical environment, rapid heating is required to reduce the effects of thermal diffusion and motion.

IV. Discussion and Future Work

The feasibility of monitoring the progression of RF ablation in the myocardium using a slope change in the thermal strain curve has been demonstrated using both *in vitro* and *in vivo*

measurements in a porcine model. The speed of sound for most water-bearing tissue increases with temperature. However, at temperatures above about 50°C, there is no further increase in the sound speed and the temperature coefficient may become slightly negative. For ablation therapy, irreversible injury to tissue and a complete heart block occurs at around 48 to 50°C. Using these two properties, we propose a potential tool to detect the moment at which clinically significant tissue damage occurs by using the reduced slope in the thermal strain as a function of heating time.

The variation in sound speed with temperature for most water-bearing soft tissue follows a similar pattern to that of water. Around 37°C, the thermal expansion coeffcient for water bearing tissue is negligible compared with the sound speed variation with temperature. However, at temperatures above about 50°C, there is no further increase in the sound speed. At this point, thermal expansion can contribute to physical displacements at the same level as sound speed variations to apparent displacements. Thus, TSI may not be practical for ablation monitoring based on precise temperature measurements, because it is more sensitive and unambiguous for small temperature changes in the range below 50°C. For ablation treatment of arrhythmia, however, a robust, reproducible indicator of tissue necrosis rather than absolute temperature monitoring is required. In particular, it is more important to know when tissue temperature has reached or exceeded 50°C so ablation can be terminated.

For the first time, a specially equipped ablation tip ML ICE array was used to collect thermal strain data during RF ablation in the right atrium of the beating heart *in vivo*. Similar to *in vitro* results, the thermal strain curve plateaus around 50°C. For this initial *in vivo* experiment, ECG triggering was not integrated with data acquisition because of a weak ECG signal that was overwhelmed by the RF ablation signal. Therefore, ultrasound data were acquired continuously and manually processed to identify image frames that would be used for 2-D speckle tracking.

It is desirable to automatically select both reference frames and their respective well-matched regions based on correlation coefficients. Because minimal cardiac motion occurs during end-diastole [45], this cardiac phase can be easily identified in the ECG, facilitating subsequent data collection and processing. Currently, we are investigating several options to enable ECG-triggered data acquisition. Because we were able to trigger the RF generator to start the ablation, we could use the signal from the generator fed into the ultrasound system. This technique will obviously depend on the ringdown time of the RF ablation signal. Another option would be to create a special isolation buffer amplifier for the animal ECG to provide a cleaner signal to the Vivid-7 machine.

Another issue is the low SNR of the prototype ML array. Because it has a low frame rate (1 Hz) relative to the heart rate, we did not have enough frames to average within a cycle to compensate for low SNR. However, it would be beneficial to use a higher frame rate for averaging. The speckle tracking algorithm also will benefit from a higher frame rate, which permits less mismatch and more usable frames in one cycle.

Important tissue parameters, such as the attenuation coefficient and thermal expansion coefficient, which could affect the apparent temperature rise, and thus influence speckle tracking, have not been included in this data analysis. Further studies will involve finite element simulations that will include all relevant parameters. Nevertheless, it is important to note that the goal of this technique was not to track an absolute temperature but to detect clinically significant tissue damage during ablation therapy. Other possible indices to monitor the ablation processes, such as the stiffness change in the ablated tissues compared with normal tissues, temperature dependence of the shear modulus [47], and thermally-induced changes in backscattered energy (CBE) from tissue inhomogeneities, can be used in conjunction with TSI.

These methods use the same RF data but are processed differently. In the future, we will explore the possibility of integrating these measures for robust monitoring and real-time optimization of RF ablation in the heart.

Because only three *in vivo* experiments are reported in this paper, additional *in vivo* studies are needed to better evaluate the robustness of this technique for real clinical applications. Nonetheless, preliminary results look promising and suggest that thermal strain imaging may be a useful tool to guide RF ablations of the heart using intracardiac devices.

References

1. Jackman WM, Wang X, Friday KJ, Roman CA, Moulton KP, Beckman KJ, McClelland JH, Twidale N, Hazlitt HA, Prior MI, Margolis PD, Calame JD, Overholt ED, Lazzara R. Catheter ablation of accessory atrioventricular pathways (Wolff-Parkinson-White Syndrome) by radiofrequency current. N. Engl. J. Med. 1991 Jun. 6.vol. 324:1605–1611. [PubMed: 2030716]
2. Calkins H, Prystowsky E, Carlson M, Klein LS, Saul JP, Gillette P. Temperature monitoring during radiofrequency catheter ablation procedures using closed loop control. Circulation. 1994; vol. 90(no. 3):1279–1286. [PubMed: 8087936]
3. Lesh MD, Van Hare GF, Schamp DJ, Chien W, Lee MA, Griffin JC, Langberg JJ, Cohen TJ, Lurie KG, Scheinman MM. Curative percutaneous catheter ablation using radiofrequency energy for accessory pathways in all locations: Results in 100 consecutive patients. J. Am. Coll. Cardiol. 1992; vol. 19(no. 6):1303–1309. [PubMed: 1564231]
4. Kugler JD, Danfrod DA, Deal BJ, Gillette PC, Perry JC, Silka MJ, Van Hare GF, Walsh EP. Radiofrequency catheter ablation for tachyarrhythmias in children and adolescents. N. Engl. J. Med. 1994; vol. 330(no. 21):1481–1487. [PubMed: 8164700]
5. Pappone C, Francesco M, Santinelli R, Vicedomini G, Sala S, Paglino G, Mazzone P, Lang CC, Gulletta S, Augello G, Santinelli O, Santinelli V. Radiofrequency ablation in children with asymptomatic Wolff–Parkinson–White syndrome. N. Engl. J. Med. 2004; vol. 351(no. 12):1197–1205. [PubMed: 15371577]
6. Epstein LM, Chiesa N, Wong MN, Lee RJ, Griffin JC, Scheinman MM, Lesh MD. Radiofrequency catheter ablation in the treatment of supraventricular tachycardia in the elderly. J. Am. Coll. Cardiol. 1994; vol. 23(no. 6):1356–1362. [PubMed: 8176093]
7. Peters NS, Schilling RJ, Kangaratnam P, Markides V. Atrial fibrillation: Strategies to control, combat, and cure. Lancet. 2002; vol. 359(no. 9306):593–603. [PubMed: 11867130]
8. Zivin, A.; Strickberger, SA. Temperature monitoring versus impedance monitoring during RF catheter ablation. In: Huang, SK.; Wilber, DJ., editors. Radiofrequency Catheter Ablation of Cardiac Arrhythmias: Basic Concepts and Clinical Applications. Mount Kisco, NY: Futura; 1994.
9. Schwartzman D, Michele JJ, Trankiem CT, Ren JF. Electrogram-guided radiofrequency catheter ablation of atrial tissue comparison with thermometryguide ablation: comparison with thermometry-guide ablation. J. Interv. Card. Electrophysiol. 2001; vol. 5(no. 3):253–266. [PubMed: 11500580]
10. Langberg JJ, Harvey M, Calkins H, el-Atassi R, Kalbfleisch SJ, Morady F. Titration of power output during radiofrequency catheter ablation of atrioventricular nodal reentrant tachycardia. Pacing Clin. Electrophysiol. 1993; vol. 16(no. 3):465–470. [PubMed: 7681198]
11. Langberg JJ, Calkins H, el-Atassi R, Borganelli M, Leon A, Kalbfleisch SJ, Morady F. Temperature monitoring during radiofrequency catheter ablation of accessory pathways. Circulation. 1992; vol. 86(no. 5):1469–1474. [PubMed: 1423961]
12. Eick OJ, Bierbaum D. Tissue temperature-controlled radiofrequency ablation. Pacing Clin. Electrophysiol. 2003; vol. 26(no. 3):725–730. [PubMed: 12698673]
13. Nath S, Lynch C, Whayne JG, Haines DE. Cellular electrophysiologic effects of hyperthermia on isolated guinea pig papillary muscle: Implications for catheter ablation. Circulation. 1993; vol. 88 (no. 4):1826–1831. [PubMed: 8403328]
14. Haines DE, Watson DD. Tissue heating during radiofrequency catheter ablation: A thermodynamic model and observations in isolated perfused and superfused canine right ventricular free wall. Pacing Clin. Electrophysiol. 1989; vol. 12(no. 6):962–976. [PubMed: 2472624]

15. Falk RH. Atrial fibrillation. N. Engl. J. Med. 2001 Apr. 5; vol. 344(no. 14):1067–1078. [PubMed: 11287978]
16. Haines DE, Verow AF. Observations on electrode-tissue interface temperature and effect on electrical impedance during radiofrequency ablation of ventricular myocardium. Circulation. 1990; vol. 82(no. 3):1034–1038. [PubMed: 2393987]
17. Hindricks G, Haverkamp W, Gulker H, Rissel U, Budde T, Richter KD, Borggrefe M, Breithardt G. Radiofrequency coagulation of ventricular myocardium: improved prediction of lesion size by monitoring catheter tip temperature. Eur. Heart J. 1989; vol. 10(no. 11):972–984. [PubMed: 2591398]
18. Shitzer A, Erez A. Controlled destruction and temperature distributions in biological tissues subjected to monoactive electrocoagulation. J. Biomech. Eng. 1980; vol. 102(no. 1):42–49. [PubMed: 7382452]
19. Organ LW. Electrophysiologic principles of radiofrequency lesion making. Appl. Neurophysiol. 1976; vol. 39(no. 2):69–76. [PubMed: 1052287]
20. Blouin LT, Marcus FI, Lampe L. Assessment of effects of radiofrequency energy field and thermistor location in an electrode catheter on the accuracy of temperature measurement. Pacing Clin Electrophysiol. 1991; vol. 14(no. 5, pt. 1):807–813. [PubMed: 1712958]
21. Wood MA, Shaffer KM, Ellenbogen AL, Ownby ED. Microbubbles during radiofrequency catheter ablation: Composition and formation. Heart Rhythm. 2005; vol. 2(no. 4):397–403. [PubMed: 15851343]
22. Varghese T, Zagzebski JA, Chen Q, Techavipoo U, Frank G, Johnson C, Wright A, Lee FT Jr. Ultrasound monitoring of temperature change during radiofrequency ablation: Preliminary in-vivo results. Ultrasound Med. Biol. 2002; vol. 28(no. 3):321–329. [PubMed: 11978412]
23. Ueno S, Hashimoto M, Fukukita H, Yano T. Ultrasound thermometry in hyperthermia. Proc. IEEE Ultrasonics Symp. 1990:1645–1652.
24. Arthur RM, Straube WL, Trobaugh JW, Moros EG. Non-invasive estimation of hyperthermia temperatures with ultrasound. Int. J. Hyperthermia. 2005; vol. 21(no. 6):589–600. [PubMed: 16147442]
25. Nasoni, R.; Bowen, T. Ultrasonic speed as a parameter for non-invasive thermometry. In: Mizushina, S., editor. Non-Invasive Temperature Measurement. Vol. vol. 1. New York, NY: Gordon and Breach; 1989. p. 95-107.
26. Seip R, Ebbini ES. Noninvasive estimation of tissue temperature response to heating fields using diagnostic ultrasound. IEEE Trans. Biomed. Eng. 1995; vol. 42(no. 8):828–839. [PubMed: 7642197]
27. Maass-Moreno R, Damianou CA. Noninvasive temperature estimation in tissue via ultrasound echo-shifts, Part I. Analytical model. J. Acoust. Soc. Am. 1996; vol. 100(no. 4):2514–2521. [PubMed: 8865654]
28. Maass-Moreno R, Damianou CA, Sanghvi NT. Noninvasive temperature estimation in tissue via ultrasound echo-shifts, Part II. In vitro study. J. Acoust. Soc. Am. 1996; vol. 100(no. 4):2522–2530. [PubMed: 8865655]
29. Shi Y, Witte RS, Milas SM, Neiss JH, Chen XC, Cain CA, O'Donnell M. Microwave-induced thermal imaging of tissue dielectric properties. Ultrason. Imaging. 2003; vol. 25(no. 2):109–121. [PubMed: 12924532]
30. Shi Y, Witte RS, O'Donnell M. Identification of vulnerable atherosclerotic plaque using IVUS-based thermal strain imaging. IEEE Trans. Ultrason. Ferroelectr. Freq. Control. 2005; vol. 52(no. 5):844–850. [PubMed: 16048186]
31. Pereira FR, Machado JC, Foster FS. Ultrasound characterization of coronary artery wall in vitro using temperature dependent wave speed. IEEE Trans. Ultrason. Ferroelectr. Freq. Control. 2003; vol. 50 (no. 11):1474–1485. [PubMed: 14682631]
32. Kim K, Huang SW, Hall TL, Witte RS, Chenevert TL, O'Donnell M. Arterial vulnerable plaque characterization using ultrasound-induced thermal strain imaging (TSI). IEEE Trans. Biomed. Eng. 2008; vol. 55(no. 1):171–180. [PubMed: 18232359]
33. Bamber JC, Hill CR. Ultrasonic attenuation and propagation speed in mammalian tissues as a function of temperature. Ultrasound Med. Biol. 1979; vol. 5(no. 2):149–157. [PubMed: 505616]

34. Pernot M, Tanter M, Bercoff J, Waters KR, Fink M. Temperature estimation using ultrasonic spatial compound imaging. IEEE Trans. Ultrason. Ferroelectr. Freq. Control. 2004; vol. 51(no. 5):606–615. [PubMed: 15217237]
35. Souchon R, Bouchoux G, Maciejko E, Lafon C, Cathignol D, Bertrand M, Chapelon JY. Monitoring the formation of thermal lesions with heat-induced echo-strain imaging: A feasibility study. Ultrasound Med. Biol. 2005; vol. 31(no. 2):251–259. [PubMed: 15708465]
36. Miller NR, Bamber JC, Ter Haar GR. Imaging of temperature-induced echo strain: Preliminary in vitro study to assess feasibility for guiding focused ultrasound surgery. Ultrasound Med. Biol. 2004; vol. 30(no. 3):345–356. [PubMed: 15063516]
37. Stephens DN, Cannata J, Liu R, Zhao JZ, Shung KK, Nguyen H, Chia R, Dentinger A, Wildes D, Thomenius KE, Mahajan A, Shivkumar K, Kim K, O'Donnell M, Nikoozadeh A, Oralkan O, Khuri-Yakub PT, Sahn DJ. Multifunctional catheters combining intracardiac ultrasound imaging and electrophysiology sensing. IEEE Trans. Ultrason. Ferroelectr. Freq. Control. 2008; vol. 55(no. 7): 1570–1581. [PubMed: 18986948]
38. Stephens DN, O'Donnell M, Thomenius KE, Dentinger A, Wildes D, Chen P, Shung KK, Cannata J, Khuri-Yakub PT, Oralkan O, Mahajan A, Shivkumar K, Sahn DJ. Experimental studies with a 9f forward-looking intracardiac imaging and ablation catheter. J. Ultrasound Med. 2009; vol. 28(no. 2): 207–215. [PubMed: 19168770]
39. Meaney PM, Clarke RL, ter Haar GR, Rivens IH. A 3-D finite-element model for computation of temperature profiles and regions of thermal damage during focused ultrasound surgery exposures. Ultrasound Med. Biol. 1998; vol. 24(no. 9):1489–1499. [PubMed: 10385970]
40. Pennes M. Analysis of tissue and arterial blood temperature in the resting human forearm. J. Appl. Physiol. 1948; vol. 1(no. 2):93–122. [PubMed: 18887578]
41. Duck, FA. Physical Properties of Tissue: A Comprehensive Reference Book. London, UK: Academic; 1990.
42. Hynynen K, DeYoung D, Kundrat M, Moros E. The effect of blood perfusion rate on the temperature distributions induced by multiple, scanned and focused ultrasonic beams in dogs' kidneys *in vivo*. Int. J. Hyperthermia. 1989; vol. 5(no. 4):485–497. [PubMed: 2746052]
43. D'Hooge J, Heimdal A, Jamal F, Kukulski T, Bijnens B, Rademakers F, Hatle L, Suetens P, Sutherland GR. Regional strain and strain rate measurements by cardiac ultrasound: Principles, implementation and limitations. Eur. J. Echocardiogr. 2000; vol. 1(no. 3):154–170.
44. Konofagou EE, D'Hooge J, Ophir J. Myocardial elastography—A feasibility study in vivo. Ultrasound Med. Biol. 2002; vol. 28(no. 4):475–482. [PubMed: 12049961]
45. de Korte CL, Carlier SG, Mastik F, Doyley MM, van der Steen AF, Serruys PW, Bom N. Morphological and mechanical information of coronary arteries obtained with intravascular elastography: Feasibility study in vivo. Eur. Heart J. 2002; vol. 23(no. 5):405–413. [PubMed: 11846498]
46. Lubinski MA, Emelianov SY, O'Donnell M. Speckle tracking methods for ultrasonic elasticity imaging using short time correlation. IEEE Trans. Ultrason. Ferroelectr. Freq. Control. 1999; vol. 46 (no. 1):82–96. [PubMed: 18238401]
47. Sapin-de Brosses E, Gennisson JL, Pernot M, Fink M, Tanter M. Temperature dependence of the shear modulus of soft tissues assessed by ultrasound. Phys. Med. Biol. 2010; vol. 55(no. 6):1701–1718. [PubMed: 20197599]

Biographies

Chi Hyung Seo (S'04–M'09) received her B.S. degree in computer engineering from the University of Waterloo, Waterloo, ON, Canada, in 1997, and her M.S. and Ph.D. degrees in biomedical engineering from the University of Southern California, Los Angeles, CA, in 2006 and 2008, respectively. From 2009 to 2010, she was appointed as a Senior Fellow of the Bioengineering department at the University of Washington, Seattle, WA. Her research area includes signal processing, beamforming, 2-D array design, thermal strain imaging, elasticity imaging, photoacoustic imaging, and catheter based devices. Currently, she is a Systems Engineer at Siemens Healthcare, Issaquah, WA.

Douglas N. Stephens (M'82) received the B.S. degree in physiology from the University of California, Davis in 1976, and the B.S. and M.S. degrees in electrical and electronic engineering and biomedical engineering in 1981 and 1983, respectively, from California State University, Sacramento. In early 1985, he joined the pioneering technical group at EndoSonics Corporation. As a key contributor at EndoSonics in solid state intravascular ultrasound (IVUS) technology, he was responsible for all catheter electronics and analog signal processing. In 1990, Mr. Stephens led the technical effort in the creation of the world's first commercial 3.5-F solid-state ultrasound imaging catheter and was awarded the first EndoSonics Fellowship Award in that year. As vice-president of strategic technology at EndoSonics and Jomed, he was responsible for new designs of IVUS solid-state technology. Mr. Stephens is currently in the department of Biomedical Engineering at the University of California, Davis. He is now working on methods of ultrasound- and EM-based targeted imaging and liposome-mediated drug delivery, and provides engineering design and management for a multisite research partnership developing novel intracardiac imaging catheters for use in electrophysiology procedures. He holds nine patents in the field of medical ultrasound.

Jonathan M. Cannata (S'01–M'04) received his B.S. degree in bioengineering from the University of California at San Diego in 1998, and his M.S. and Ph.D. degrees in bioengineering from The Pennsylvania State University, University Park, PA, in 2000 and 2004, respectively.

Since 2001, he has served as the manager for the NIH Resource on Medical Ultrasonic Transducer Technology, which is currently located at the University of Southern California (USC). In 2005, he was awarded the title of Research Assistant Professor of Biomedical Engineering at USC. His current interests include the design, modeling, and fabrication of ultrasonic transducers and transducer arrays for medical applications.

Aaron M. Dentinger (M'95) received his B.S. degree in engineering physics in 1992 and his M.S. and Ph.D. degrees in electrical engineering in 1994 and 2006, respectively, from Rensselaer Polytechnic Institute, Troy, NY.

Since 1995, he has worked as an Electrical Engineer at GE Global Research in Niskayuna, NY and is currently a member of the Ultrasound and Biomedical Laboratory. Prior to joining GE, he was employed at Reveo, Inc. His current research interests are in ultrasound signal and image processing for vascular, cardiac, and physiological measurements.

Feng Lin (M'01) received his B.E. degree in 1993 from the Department of Electrical Engineering at Southeast University, Nanjing, China, the M.E. degree in 1996 from the Department of Automation at Tsinghua University, Beijing, China, and the Ph.D. degree in 2001 from the Department of Electrical and Computer Engineering at the University of Rochester, Rochester, NY. Since March 2001, he has been with General Electric Company, where he was Ultrasound Systems Engineer at GE Healthcare in Milwaukee, WI, from 2001 to 2005; Ultrasound/Biomedical Scientist at GE Global Research Center in Niskayuna, NY, from 2005 to 2010; and is currently Principal Engineer at GE Healthcare in Wuxi, China.

His research interests include ultrasound tomography, adaptive beamforming, elasticity imaging, ultrasound-guided therapy, and biomedical applications of signal and image processing.

Suhyun Park was born in Seoul, Korea, in 1977. She received the B.S. and M.S. degrees in electrical engineering from the Ewha Women's University, Seoul, South Korea, in 1999 and 2001, respectively. From 2001 to 2003, she was with Mediaexcel, Austin, TX, as a software engineer, where she developed video codecs. In 2008, she earned a Ph.D. degree in biomedical engineering from the University of Texas at Austin, Austin, TX, then joined GE Global Research, Niskayuna, NY, as an electrical engineer. Her research has focused on various applications on ultrasound imaging including beamforming, elastography, and photoacoustic imaging. Recently, she has been leading projects on ultrasound contrast imaging using nonlinear responses in contrast agents.

Douglas Wildes received a B.A. degree in physics and mathematics from Dartmouth College in 1978 and M.Sc. and Ph.D. degrees in physics from Cornell University in 1982 and 1985, then joined GE Global Research in Niskayuna, NY. Since 1991, his research has focused on aperture design, fabrication processes, and high-density interconnect technology for multi-row and 4-D imaging transducers for medical ultrasound. Dr. Wildes has 31 issued patents and 24 external publications. He is a member of the American Physical Society and a Senior Member of IEEE.

Kai E. Thomenius (M’66) was awarded the B.S., M.S., and Ph.D. degrees in electrical engineering and physiology from Rutgers University, New Brunswick, NJ, in 1968, 1970, and 1978, respectively. His background includes both academic and industrial activities, including teaching at Rutgers University, Stevens Institute of Technology, Hoboken, NJ, and Rensselaer Polytechnic Institute (RPI), Troy, NY. He has worked for the U.S. Army Electronics Command at Ft. Monmouth, NJ, as an RF engineer. He has held research-related positions in medical ultrasound since 1976 for Picker Ultrasound, Northford, CT, Elscint, Inc., Boston, MA, ATL/Interspec, Ambler, PA, and most recently GE Global Research in Niskayuna, NY, where he is currently a Chief Technologist in the Imaging Technologies Organization. In addition, he is an adjunct professor in the Electrical, Computer, and Systems Engineering Department at RPI. The focus of his industrial work has centered on ultrasound systems design, especially beamformation, miniaturization of ultrasound scanners, ultrasound bioeffects, and the design

for ultraportable imagers. An additional focus deals with novel application of ultrasonic imagers; an example of this is the current publication relating to measurement of cardiovascular parameters using ultrasound.

Dr. Thomenius is a Fellow of the American Institute of Ultrasound in Medicine (AIUM), a member of the American Association of Physicists in Medicine, the American Society for Echocardiography, the Acoustical Society of America, and the Society of Photo-Optical Instrumentation Engineers (SPIE). He is a member of the editorial board of the *Ultrasonic Imaging* iournal and serves as a reviewer of grant proposal for the National Institutes of Health and of articles for several ultrasound journals. In addition, he serves in the Technical Program Committees for IEEE Ultrasonics Symposium, the annual conference of the AIUM, and the Medical Imaging Conference of the SPIE.

Peter Chen has more than 30 years of experience in the medical device industry. He was the Founder of Irvine Biomedical, Inc. (IBI). Through innovation, new product developments, and superior product quality, IBI became one of the most successful medical device companies in the US owned by a Chinese-American. Dr. Chen established IBI in 1995, and successfully led the company to develop, launch, and market new electrophysiology products around the world. He was able to grow IBI into a multi-million dollar company before being acquired by St. Jude Medical, one of the largest global medical device companies, in 2004. After the acquisition, Dr. Chen continued his position as the President of IBI and led the company to increase its business at 33% annually and to generate a revenue of over $110 million in 2008. Today, 7 years after the acquisition, IBI's product brand name is still the best-known brand name in the St. Jude Medical's electrophysiology product line.

Dr. Chen is well known in the field of electrophysiology and cardiac rhythm management through his innovative invention of new devices for treating cardiac arrhythmias. He is the

author and co-author of more than 17 patents and 23 publications. In 2009, based on his success with IBI and on his contribution to the St. Jude Medical business, Dr. Chen was named as the President of a newly created division, Center for Innovation and Strategic Collaboration, a corporate research and development center of St. Jude Medical.

Dr. Chen was born in China and grew up in Taiwan. He obtained his master's degree in electrical engineering from the University of Kansas and earned his Ph.D. degree in biomedical engineering from Rutgers, the State University of New Jersey.

Prior to founding IBI, Dr. Chen held several key R & D positions in some of the major medical device companies, including Baxter Health Care, Guidant Corp, Chiron, and Johnson & Johnson.

Dr. Chen was named twice in the 2006–2007 Strathmore's Who's Who. He was also named as Honorary Chairman of the Business Advisory Council of The National Republic Congressional Committee in 2003 and 2007. Dr. Chen is very involved in various activities of medical industry and biomedical society in southern California. He served on the Board of Directors of several medical device companies and medical associations. Dr. Chen is an active Advisory Member of the Sino-American Biomedical & Pharmaceutical Professional Association (SABPA) and frequently speaks at the annual conference of this organization as well as at the ASME frontiers in Biomedical Devices Conference. Dr. Chen was the latest recipient of 2011 Achievement Award of Chinese-American Engineers and Scientists Association of Southern California. He also presents papers and speaks at various medical conferences around the world from time to time.

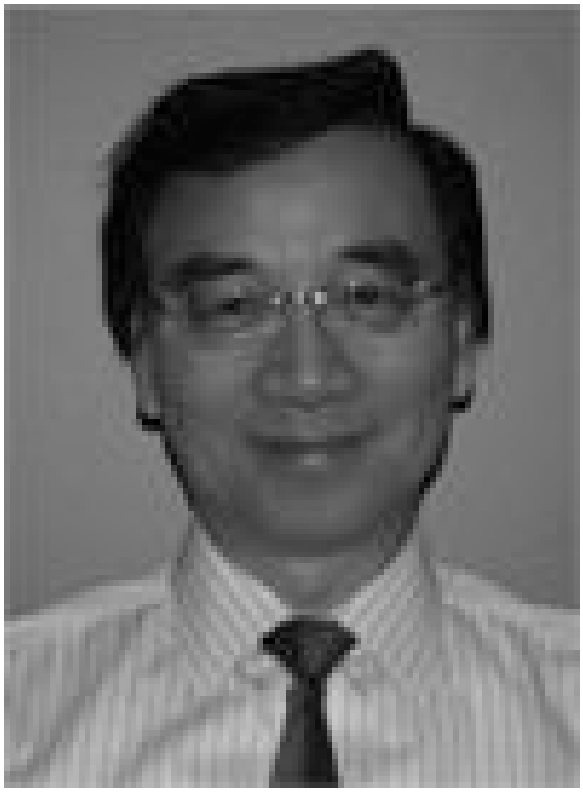

Tho Hoang Nguyen was born in Cho Lon, Vietnam. He received a B.S. degree in electrical engineering from the California State University–Fullerton, Fullerton, CA. He works for ST. Jude Medical, Inc. He is an R&D engineer and is responsible for instrumentation design and

development. His present position is Principal Engineer. He has received 5 patents in medical devices under St. Jude Medical, Inc.

Alan de La Rama received his B.S. degree in mechanical engineering from the University of San Carlos, Philippines in 1980. In 1983, he joined American Hospital Supply Corp. (AHSC) where he was involved in designing medical devices such as laser surgical tools, endoscopes, and laparoscopic devices. Shortly thereafter, Baxter Healthcare acquired AHSC, and he expanded his design responsibilities to cover all minimally invasive devices such as catheters, retrival devices, and other cardiovascular products. From 1991 to 1994, he consulted with Optical Radiation Corp. (ORC), where he was involved in designing a mechanical cornea reshaping tool for myopia patients. He also did some consulting with SpectrumMed, where he designed trachea endoscopes to assist endotracheal tube placement.

In 1994, he joined Irvine Biomedical Inc. (IBI), a start-up company that designs and develops products for interventional cardiac electrophysiology. He was the key contributor to all EP products from conceptual to product market release. In 2004, St. Jude Medical Corporation acquired IBI, and he continued to lead the Research and Development group as Director of R&D. Currently, he supports the St. Jude Medical research group as a Senior Director of Technology Development.

Jong Seob Jeong (S’00–M’10) was born in Seoul, South Korea, on February 5, 1976. He received his B.S. and M.S. degrees in electronic engineering from Sogang University, Seoul, South Korea in 1999 and 2001, respectively, and a Ph.D.degree in biomedical engineering from the University of Southern California, Los Angeles, CA in 2010. From 2001 to 2005, he worked at the Telecommunication Research and Development Center, Samsung Electronics Co., Ltd., Kyunggido, South Korea, where he participated in the development of the WCDMA wireless communication system. From 2010 to 2011, he pursued post-doctoral research at the NIH Resource Center for Medical Ultrasonic Transducer Technology, Department of Biomedical Engineering, University of Southern California, Los Angeles, CA. He is currently an assistant professor in the Department of Medical Biotechnology, College of Life Science and Biotechnology, Dongguk University-Seoul, Seoul, South Korea. His research interests are medical signal processing and design, modeling, and fabrication of ultrasonic single-element and array transducers for diagnosis and therapy.

Aman Mahajan obatined his M.D. degree from the University of Delhi Medical School in New Delhi, India in 1991, and a Ph.D. degree from the Dept. of Physiology, UCLA School of Medicine and Health Sciences, Los Angeles, CA, in 2005. He is currently an Associate Clinical Professor Cardiac Anesthesiology in the Department of Anesthesiology, UCLA Medical Center, UCLA School of Medicine and Health Sciences. Dr. Mahajan is a member of numerous professional societies and has interests in the areas of arrhythmia biology and stem cell electrophysiology.

Kalyanam Shivkumar received his medical degree from the University of Madras, India, in 1991 and his Ph.D. degree from University of California, Los Angeles (UCLA), in 2000. He completed his cardiology fellowship training at UCLA, and on completion of his training joined the faculty at University of Iowa, where he also served as the associate director of cardiac electrophysiology. In 2002, he was recruited back to UCLA to direct the newly created UCLA Cardiac Arrhythmia Center at the David Geffen School of Medicine at UCLA. His field of specialization is interventional cardiac electrophysiology, and he heads a group at UCLA that is involved in developing innovative techniques for the nonpharmacological management of cardiac arrhythmias. He is an associate professor of medicine and holds a joint appointment in the Department of Radiology at UCLA. Dr. Shivkumar is certified by the American Board of Internal Medicine in the subspecialties of cardiovascular disease and clinical cardiac electrophysiology. He holds memberships in several professional organizations, including the American Heart Association, American College of Cardiology, and the Heart Rhythm Society.

Amin Nikoozadeh received the B.S. degree from Sharif University of Technology, Tehran, Iran, in 2002, the M.S. degree from Stanford University, Stanford, CA, in 2004, and the Ph.D. degree from Stanford University, Stanford, CA, in 2010, all in electrical engineering. For his Ph.D., he designed and developed fully-integrated ultrasound imaging catheters for forward-viewing intracardiac imaging using capacitive micromachined ultrasonic transducers (CMUTs).

Since 2011, he has worked as an engineering research associate at the E. L. Ginzton Laboratory of Stanford University, Stanford, CA. His past and present research interests include medical ultrasound imaging, image-guided therapeutics, MEMS, and analog circuit design, with a main focus on design, modeling, fabrication and integration of CMUTs. His current research focuses on the implementation of fully-integrated CMUT arrays for catheter-based medical imaging applications and the development of novel CMUT structures for improved performance.

Omer Oralkan joined the research staff at the E. L. Ginzton Laboratory of Stanford University in 2004 as an Engineering Research Associate. He was promoted to the rank of Senior Research Associate in 2007. He also serves as an Adjunct Faculty Member in the Department of Electrical Engineering at Santa Clara University, Santa Clara, CA. His current research focuses on the design and implementation of integrated systems for ultrasound imaging and therapy, photoacoustic imaging, chemical and biological sensor arrays, and ultrasound neural stimulation.

Dr. Oralkan has authored and co-authored moer than 100 publications and received the 2002 Outstanding Paper Award of the IEEE Ultrasonics, Ferroelectrics, and Frequency Control Society. He is a Senior Member of the IEEE.

Uyen Truong earned her B.S. degree at the University of California, Los Angeles, and subsequently, her M.D. degree at the University of California, San Diego. She trained as a Pediatric Cardiologist at Children's National Medical Center, and went on to complete a fourth-year fellowship in advanced imaging at Lucile Packard Children's Hospital. In addition, she joined Dr. David Sahn's research team at Oregon Health and Science University, where she studied the cardiomechanics of various single-ventricle hearts using advanced ultrasound and MRI techniques. She is currently an assistant professor at The Children's Hospital, University of Colorado, in Aurora, CO.

David J. Sahn was raised in New York and received his M.D. degree from Yale University cum laude in 1969. Following his medical internship at Yale, he completed his residency in Pediatric Cardiology at the University of California, San Diego in 1973 and accepted positions at the University of Arizona as Assistant Professor of Pediatric Cardiology in 1974, and Professor in 1981. From 1983 to 1992, he held positions as Professor of Pediatrics and Radiology and Chief, Division of Pediatric Cardiology, UCSD School of Medicine, La Jolla, CA. In 1992, he moved to Oregon Health & Science University in Portland, OR, where he currently holds positions as Professor of Pediatrics, Diagnostic Radiology, Obstetrics & Gynecology and Biomedical Engineering, as well as Director, Interdisciplinary Program in Cardiac Imaging.

Dr. Sahn has served on numerous professional journal editorial boards including the American Heart Association journal *Circulation*, *Journal of the American College of Cardiology*, *American Journal of Cardiology*, and *Journal of the American Society of Echocardiography*. He has served on two NIH study sections in Diagnostic Radiology and Medical Imaging and is currently a member of the NHLBI Board of Scientific Councilors. He has been the recipient of numerous honors and awards during his storied career, and is an author in more than 370 peer-reviewed publications.

Butrus T. Khuri-Yakub (F'95) received the B.S. degree in electrical engineering from the American University of Beirut, Beirut, Lebanon, the M.S. degree in electrical engineering from Dartmouth College, Hanover, NH, and the Ph.D. degree in electrical engineering from Stanford University, Stanford, CA.

He is a Professor of electrical engineering at Stanford University. His current research interests include medical ultrasound imaging and therapy, chemical/biological sensors, micromachined ultrasonic transducers, and ultrasonic fluid ejectors.

He has authored more than 500 publications and has been the principal inventor or co-inventor of 88 U.S. and internationally issued patents. Dr. Khuri-Yakub was the recipient of the Medal of the City of Bordeaux in 1983 for his contributions to nondestructive evaluation, the Distinguished Advisor Award of the School of Engineering of Stanford University in 1987, the Distinguished Lecturer Award of the IEEE Ultrasonics, Ferroelectrics, and Frequency Control Society in 1999, a Stanford University Outstanding Inventor Award in 2004, and a Distinguished Alumnus Award of the School of Engineering of the American University of Beirut, in 2005.

Matthew O'Donnell received his B.S. and Ph.D. degrees in physics from the University of Notre Dame, Notre Dame, IN, in 1972 and 1976, respectively. Following his graduate work, Dr. O'Donnell moved to Washington University in St. Louis, MO, as a postdoctoral fellow in

the Physics Department, working on applications of ultrasonics to medicine and non-destructive testing. He subsequently held a joint appointment as a Senior Research Associate in the Physics Department and a Research Instructor of Medicine in the Department of Medicine at Washington University. In 1980, he moved to General Electric Corporate Research and Development Center in Schenectady, NY, where he continued to work on medical electronics, including MRI and ultrasound imaging systems. During the 1984–1985 academic year, he was a visiting fellow in the Department of Electrical Engineering at Yale University in New Haven, CT, investigating automated image analysis systems. In 1990, Dr. O'Donnell became a Professor of Electrical Engineering & Computer Science at the University of Michigan in Ann Arbor, MI. Starting in 1997, he held a joint appointment as Professor of Biomedical Engineering. In 1998, he was named the Jerry W. and Carol L. Levin Professor of Engineering. From 1999 to 2006, he also served as Chair of the Biomedical Engineering Department. During 2006, he moved to the University of Washington in Seattle, WA, where he is now the Frank and Julie Jungers Dean of Engineering and also a Professor of Bioengineering. His most recent research has explored new imaging modalities in biomedicine, including elasticity imaging, *in vivo* microscopy, optoacoustic arrays, optoacoustic contrast agents for molecular imaging and therapy, thermal strain imaging, and catheter-based devices.

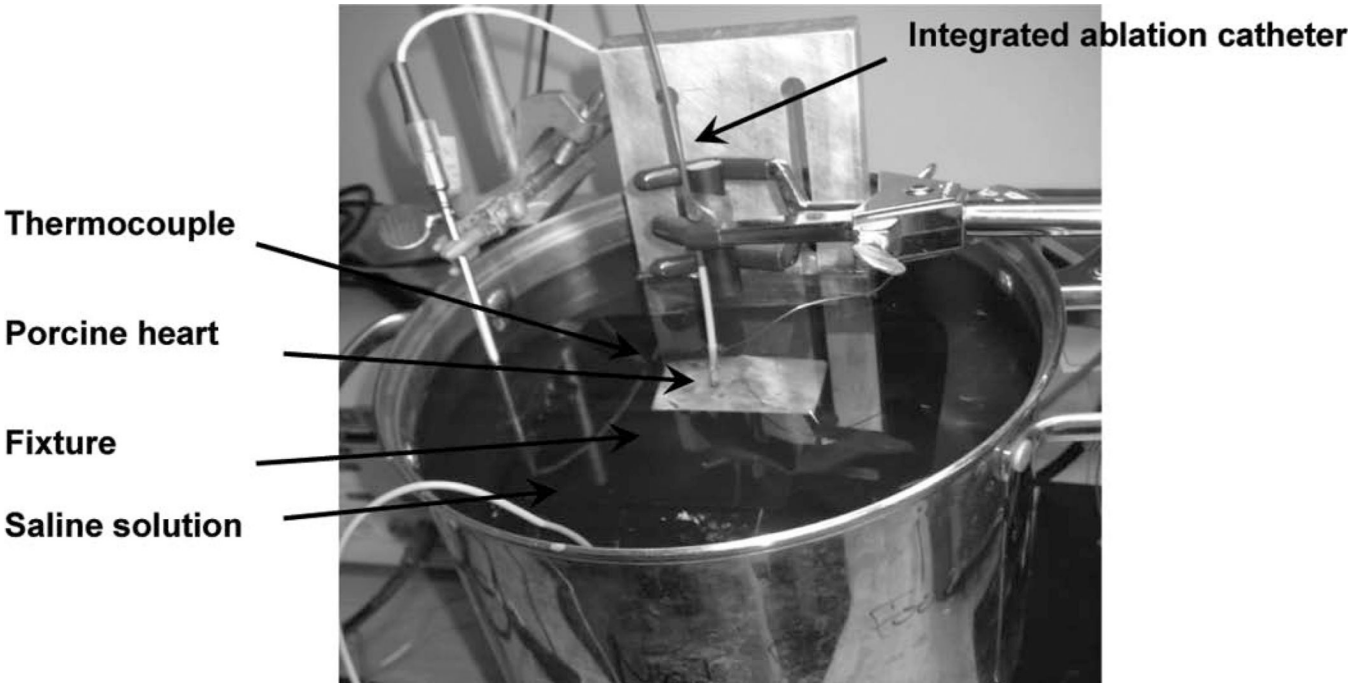

Fig. 1.
Photograph showing relative positions of the thermocouple, ablation catheter array, and the sample for the dynamic *in vitro* heating experiment.

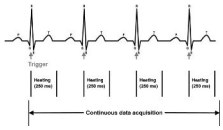

Fig. 2.
Timing diagram describing ablation/data acquisition sequence for *in vivo* experiments.

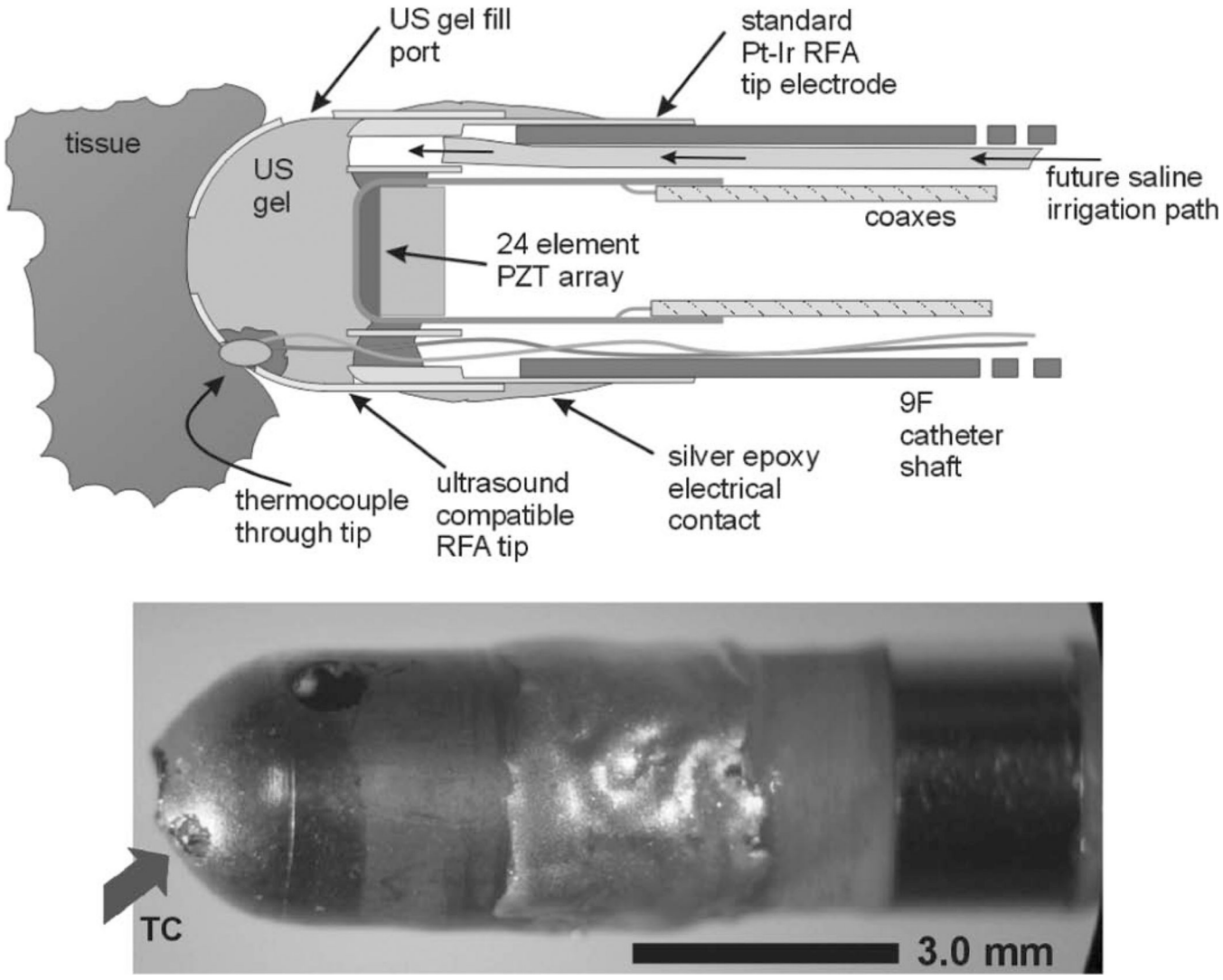

Fig. 3.

Approximate geometry of the modified microlinear-PZT catheter tip. The original microlinear-PZT tip has a special metal coated plastic which is transparent to ultrasound but permits simultaneous RF ablation. Experimental temperature feedback is performed with placement of a very small (<100 μm) thermocouple (arrow) in the plastic tip housing.

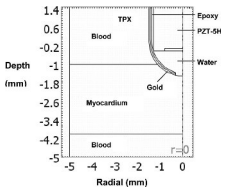

Fig. 4.
Schematic diagram of the axially symmetric region used for finite element modeling of thermal diffusion.

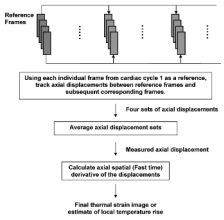

Fig. 5.
Block diagram describing processing steps to generate thermal strain image.

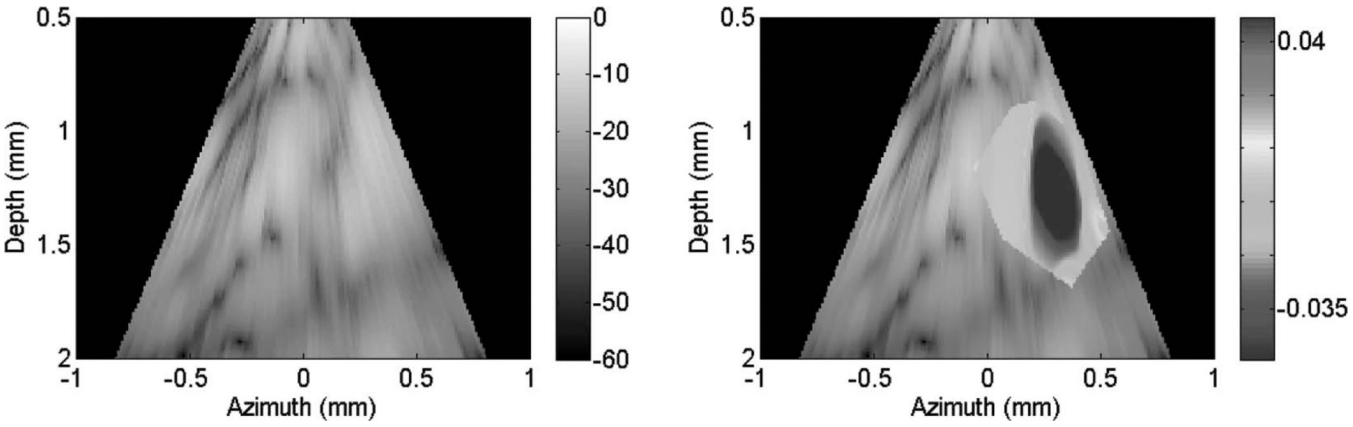

Fig. 6.

B-mode images (dB) with thermal strain overlaid using microlinear array for *in vitro* experiment: rapid heating case. Thermal strain is displayed at a temperature of approximately 52°C.

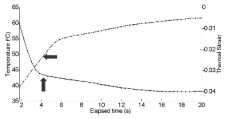

Fig. 7.

Thermal strain plotted with temperature rise in porcine myocardium using a microlinear array for *in vitro* experiment: rapid heating case.

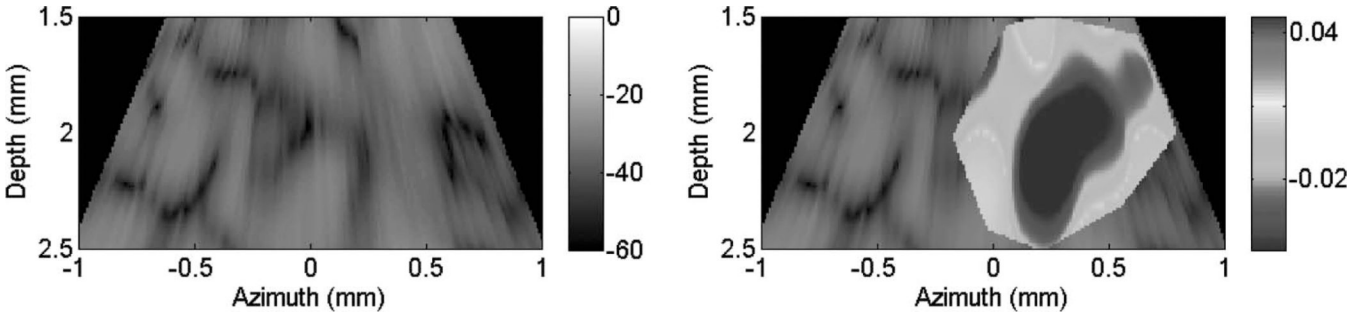

Fig. 8.

B-mode images (dB) with thermal strain overlaid using microlinear array for *in vitro* experiment: slow heating case. Thermal strain is displayed at a temperature around 52°C.

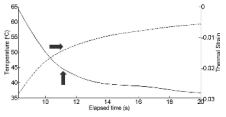

Fig. 9.
Thermal strain plotted with temperature rise in porcine myocardium using a microlinear array for *in vitro* experiment: slow heating case.

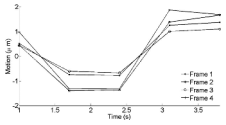

Fig. 10.
Cardiac motion versus time (first 5 cardiac cycles before RF ablation) for the same region corresponding to the thermal strain image in Fig. 11.

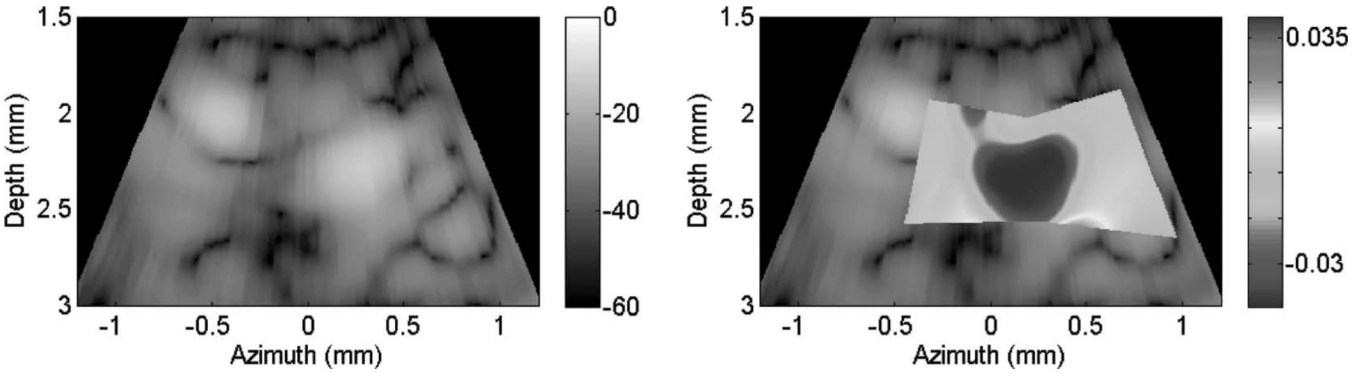

Fig. 11.

B-mode images (dB) with thermal strain overlayed using microlinear array for *in vivo* experiment: case 1. Image is displayed at time of maximum thermal strain magnitude.

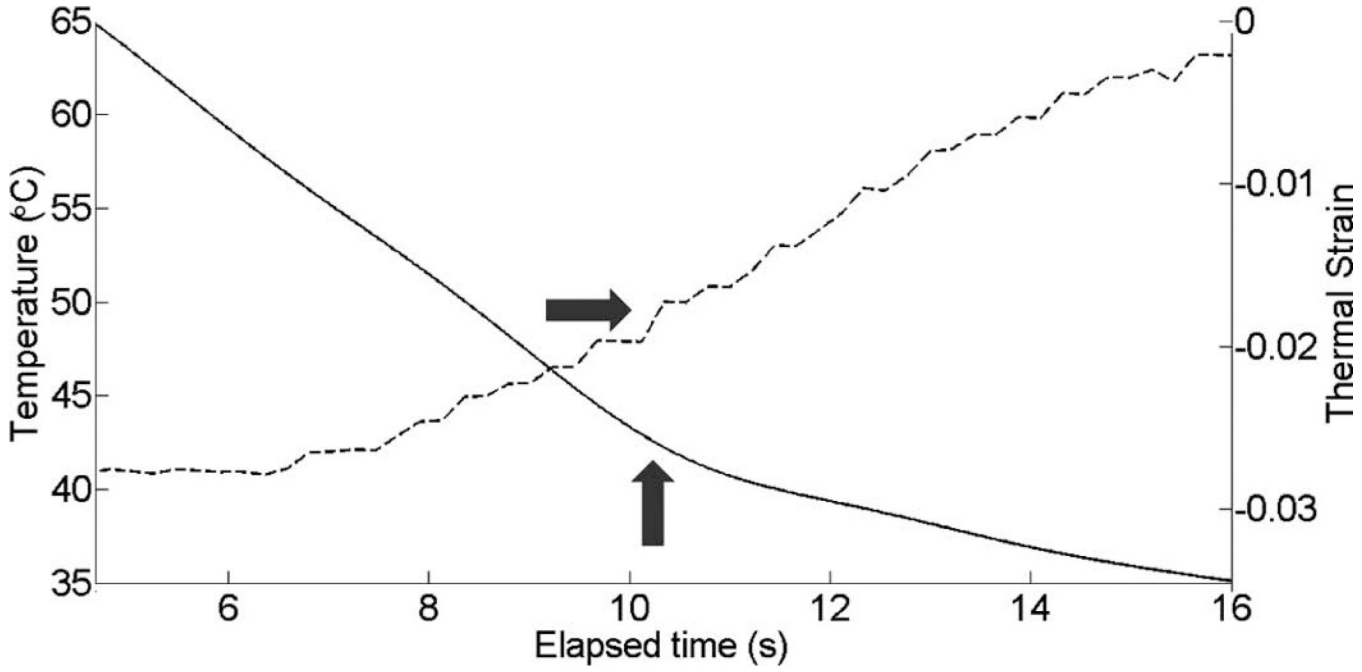

Fig. 12.
Thermal strain plotted with temperature rise in porcine myocardium using a microlinear array for *in vivo* experiment: case 1.

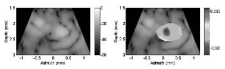

Fig. 13.
B-mode images (dB) with thermal strain overlayed using microlinear array for *in vivo* experiment: case 2. Image is displayed at time of maximum thermal strain magnitude.

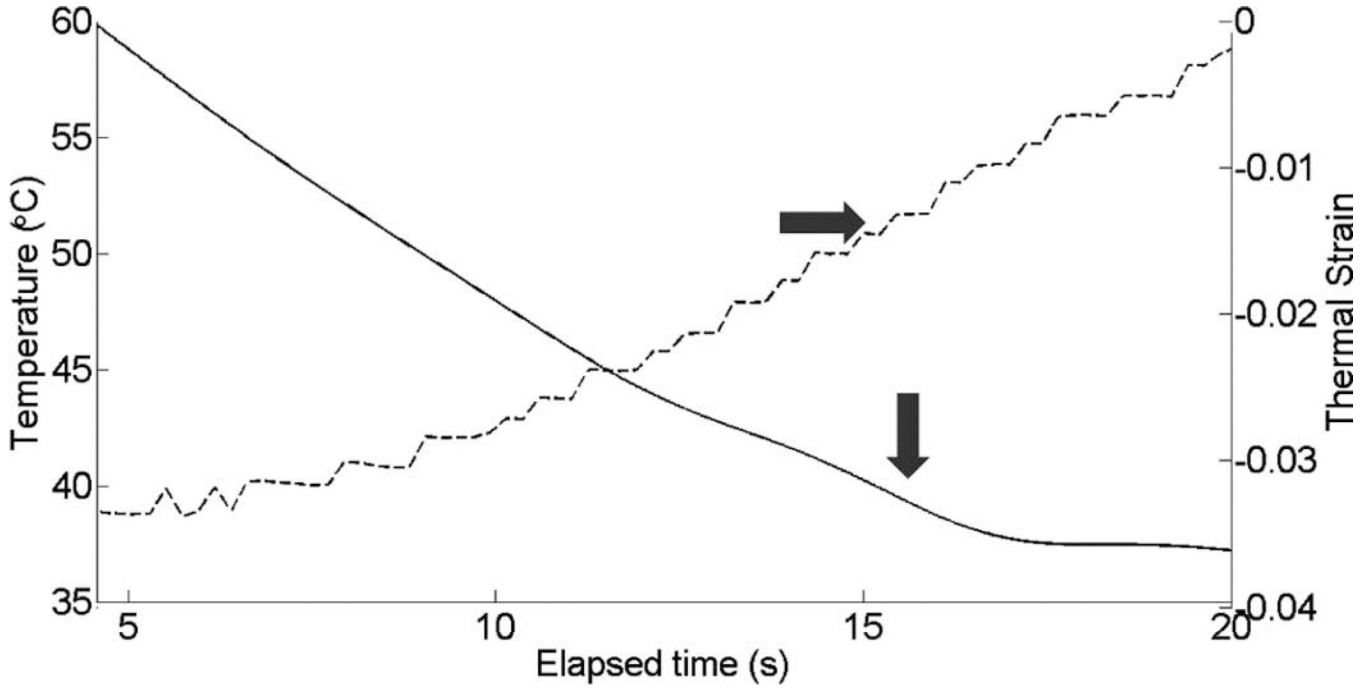

Fig. 14.
Thermal strain plotted with temperature rise in porcine myocardium using a microlinear array for *in vivo* experiment: case 2.

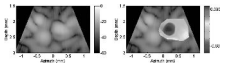

Fig. 15.
B-mode images (dB) with thermal strain overlayed using microlinear array for *in vivo* experiment: case 3. Image is displayed at time of maximum thermal strain magnitude.

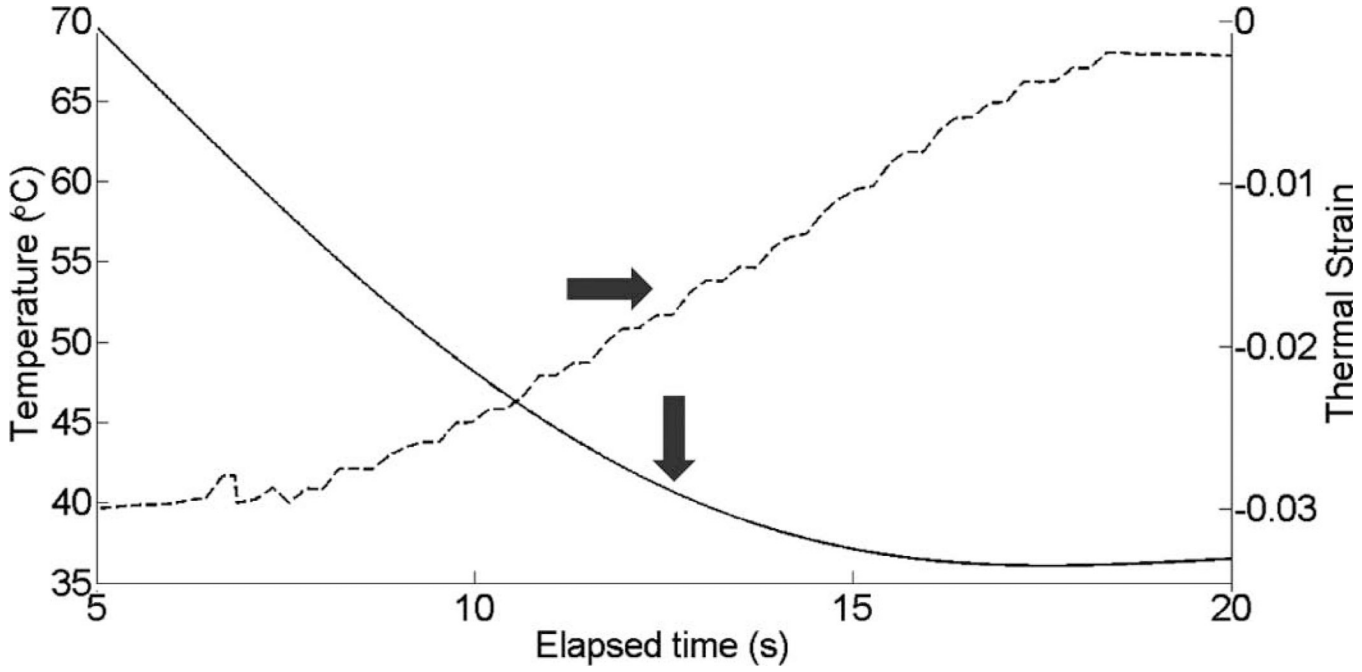

Fig. 16.
Thermal strain plotted with temperature rise in porcine myocardium using a microlinear array for *in vivo* experiment: case 3.

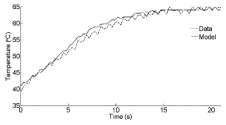

Fig. 17.
Temperature rise and thermal diffusion effect comparing measurements and finite element simulations.

TABLE I

Ultrasound System Parameters Used in Experiments.

Parameter/device description	***In vitro***	***In vivo***
Ultrasound system	GE Vivid 7, Color Doppler special mode	GE Vivid 7, Color Doppler special mode
Catheter and array	A separate ablation catheter and a prototype 9F forward-looking ML ICE catheter array	A prototype integrated ablation catheter 9F forward-looking ML ICE catheter array
Sampling frequency	20 MHz (later upsampled to 40 MHz for processing)	20 MHz (later upsampled to 40 MHz for processing)
Transmit frequency	11 MHz	11 MHz
Transmit focus	1 to 2 mm	2 mm
Imaging target	Porcine heart muscle	Porcine right atrium
Imaging depth	5 mm	10 mm
Imaging width	45°	45°
Number of beams	128	128
Packet size	8	8
Frame rate	32 Hz	1 Hz
Temperature measurement	Thermocouple	Thermocouple embedded in the array